Princeton Plasma Physics Laboratory

PPPL- 4869

PPPL- 4869

Calculation of Neoclassical Toroidal Viscosity with a Particle Simulation in the Tokamak Magnetic Braking Experiments

Kimin Kim, et. al.

April, 2013

PPPL PRINCETON PLASMA PHYSICS LABORATORY

Prepared for the U.S. Department of Energy under Contract DE-AC02-09CH11466.

Princeton Plasma Physics Laboratory
Report Disclaimers

Full Legal Disclaimer

Trademark Disclaimer

PPPL Report Availability

Princeton Plasma Physics Laboratory:

http://www.pppl.gov/techreports.cfm

Office of Scientific and Technical Information (OSTI):

http://www.osti.gov/bridge

Related Links:

U.S. Department of Energy

Office of Scientific and Technical Information

Fusion Links

Calculation of neoclassical toroidal viscosity with a particle simulation in the tokamak magnetic braking experiments

Kimin Kim
Princeton Plasma Physics Laboratory, Princeton, NJ 08543, USA

Jong-Kyu Park
Princeton Plasma Physics Laboratory, Princeton, NJ 08543, USA

Gerrit J. Kramer
Princeton Plasma Physics Laboratory, Princeton, NJ 08543, USA

Allen H. Boozer
Department of Applied Physics and Applied Mathematics, Columbia University, New York, NY 10027, USA

Jonathan E. Menard
Princeton Plasma Physics Laboratory, Princeton, NJ 08543, USA

Stefan P. Gerhardt
Princeton Plasma Physics Laboratory, Princeton, NJ 08543, USA

Nikolas C. Logan
Princeton Plasma Physics Laboratory, Princeton, NJ 08543, USA

Keith H. Burrell
General Atomics, San Diego, CA 92186, USA

Andrea M. Garofalo
General Atomics, San Diego, CA 92186, USA

Abstract. Accurate calculation of perturbed distribution function δf and perturbed magnetic field δB is essential to achieve prediction of non-ambipolar transport and neoclassical toroidal viscosity (NTV) in perturbed tokamaks. This paper reports a study of the NTV with a δf particle code (POCA) and improved understanding of magnetic braking in tokamak experiments. POCA calculates the NTV by computing δf with guiding-center orbit motion and using δB from the ideal perturbed equilibrium code (IPEC). POCA simulations are compared with experimental estimations for NTV, which are measured from angular momentum balance (DIII-D) and toroidal rotational damping rate (NSTX). The calculation shows good agreement in total NTV torque for the DIII-D discharge, where an analytic neoclassical theory also gives a consistent result thanks to relatively large aspect-ratio and slow toroidal rotations. In NSTX discharges, where the aspect-ratio is small and the rotation is fast, the theory only gives a qualitative guide for predicting NTV. However, the POCA simulation largely improves the quantitative NTV prediction for NSTX. It is discussed that a self-consistent calculation of δB using general perturbed equilibria is eventually necessary since a non-ideal plasma response can change the perturbed field and thereby the NTV torque.

1. Introduction

Toroidal symmetry braking in perturbed tokamaks can fundamentally change neoclassical transport [1, 2, 3]. Magnetic perturbations, induced by intrinsic error fields, MHD activities, and externally applied non-axisymmetric fields, distort particle orbits on deformed or broken flux surfaces, and modify the neoclassical particle transport [4]. The transport by the symmetry breaking, often called neoclassical toroidal viscosity (NTV) transport in tokamaks, is one of the essential effects of the non-axisymmetric magnetic perturbations. It provides an additional channel for toroidal momentum transport and modifies the toroidal plasma rotation, which is called magnetic braking [5, 6, 7]. Understanding and prediction of NTV and magnetic braking are important for the present and future tokamaks since small magnetic perturbations of $|\delta B/B| \sim 10^{-4}$ can dramatically change the plasma rotation to impact the macroscopic plasma stability and global performance in tokamaks [8, 9, 10].

In order to achieve a precise and self-consistent descriptions for NTV transport, two physics components should be combined; δf the perturbed distribution function and δB the non-axisymmetric magnetic field perturbations. Substantial progress has been made calculating δf and NTV by various analytical attempts [11, 12, 13, 14, 15], but they are largely limited by heavy approximations such as large aspect-ratio expansion, limitation on trapped particle effects, zero-banana-orbit width, regime separation, and simplified δB calculations. A numerical approach is eventually required for the NTV calculation in magnetic braking experiments, which should make use of a consistent δf and δB model. For this purpose, a numerical study of NTV has been performed using a δf guiding-center particle code, POCA (Particle Orbit Code for Anisotropic pressures) [4]. POCA provides improved NTV predictability by calculating δf using guiding-center orbit motions in realistic geometries and using the δB computed by IPEC (Ideal Perturbed Equilibrium Code) considering an ideal plasma response [16].

This paper presents the calculations of NTV with a particle simulation in magnetic braking experiments for DIII-D and NSTX. Section 2 describes the method to calculate δf and NTV with the particle simulation, and shows a resonant feature of NTV transport. A technique for reconstructing δB using IPEC in the experimental analysis is introduced in Sec. 3. The POCA applications for DIII-D and NSTX are presented in Sec. 4. The NTV torques, obtained from global angular momentum balance in DIII-D and estimated from rotational damping rate in NSTX, are compared with the POCA simulation and the combined NTV theory. Issues for improving the NTV prediction are discussed in Sec. 5, and the conclusions are given in Sec. 6.

2. Guiding-center particle simulation for calculation of δf and NTV

2.1. Particle code for NTV calculation

The guiding-center orbit code, POCA solves the Fokker-Planck equation with a δf Monte Carlo method to obtain the perturbed distribution function δf [4, 17]. The

Fokker-Planck equation is written as

$$\frac{d\ln f_M}{dt} + \frac{d\hat{f}}{dt} = C_m, \tag{1}$$

where the distribution function f is approximated to $f \approx f_M(1+\hat{f})$ with the local Maxwellian f_M in the fusion plasmas, and $C_m \equiv C/f$ with the pitch-angle scattering collision operator C modified to conserve the toroidal momentum [17]. The reduced Fokker-Planck equation can be rewritten as

$$\frac{d\hat{f}}{dt} = -\vec{v}\cdot\vec{\nabla}\psi\frac{\partial \ln f_M}{\partial\psi} + C_m, \tag{2}$$

then $\hat{f}$ is obtained by following

$$\begin{aligned}\Delta\hat{f} = &-\left[\frac{1}{N}\frac{\partial N}{\partial\psi} + \left(\frac{3}{2} - \frac{E}{T}\right)\frac{1}{T}\frac{\partial T}{\partial\psi}\right]\Delta\psi \\ &+ 2\nu\frac{u}{v}\lambda\Delta t - \frac{e}{T}\frac{d\Phi}{d\psi}\Delta\psi,\end{aligned} \tag{3}$$

where ν is the collision frequency, u is the parallel flow velocity, λ is the pitch-angle, and Φ is the electric potential. The first term in the right hand side of Eq. 3 represents the δf driven by particle drift motions, and the second term is the momentum correction term to preserve the toroidal momentum conservation. The last term represents the electric potential effect, which is directly related to the toroidal rotation and $\vec{E}\times\vec{B}$ precession by $E_r = -d\Phi/dr$.

The guiding-center orbit motion is tracked by the Hamiltonian orbit equations in Boozer coordinates [18]. Thus, every kind of guiding-center motion, depending on the particle's energy and pitch, magnetic field configurations, electric potential, and their combinations, is included in the POCA simulation. One example of the guiding-center drift motion is presented in Fig. 1, showing a 3D trajectory of the guiding-center without collisions in an axisymmetric NSTX plasma. As shown, the calculated guiding-center motion reflects a typical feature of the magnetic field line structures in the NSTX. In the presence of non-axisymmtric perturbations, the guiding-center orbit is distorted and drifts out faster than the axisymmetric case to drive the non-ambipolar transport and NTV as presented in Ref. [4].

The NTV torque is obtained using perturbed pressures and magnetic field spectrum [19, 20] in the POCA simulation. In Boozer coordinates, the NTV is calculated by

$$\tau_\varphi \equiv \langle \mathbf{e}_\varphi\cdot\nabla\cdot\mathbf{P}\rangle = \left\langle \frac{\delta P}{B}\frac{\partial B}{\partial\varphi}\right\rangle, \tag{4}$$

where $\mathbf{e}_\varphi = \partial\mathbf{x}/\partial\varphi$, δP is the perturbed pressures defined by $\delta P = \int d^3v(Mv_\parallel^2 + Mv_\perp^2/2)\delta f$, and the brackets denote the flux surface average. POCA has been successfully benchmarked with axisymmetric neoclassical transport theories and with the combined NTV theory [14] in the various collisionalities. Essential NTV features such as the quadratic δB dependency, the $1/\nu$ and $\nu_-\sqrt{\nu}$ behaviors, and the superbanana plateau resonances have been consistently reproduced in the zero-$\vec{E}\times\vec{B}$ limit [4].

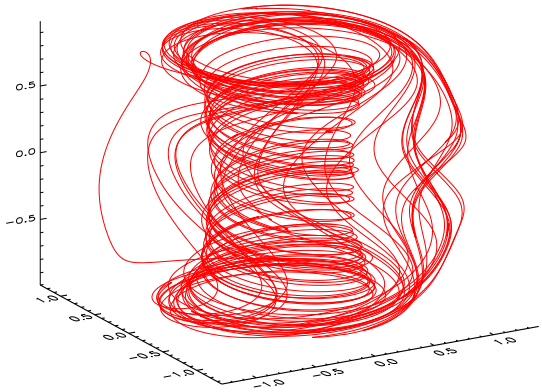

Figure 1. 3D trajectory of a single guiding-center orbit motion in an axisymmetric NSTX plasma, calculated by POCA.

2.2. Resonant nature of NTV

A well-known supposition in the magnetic braking is that the NTV is mainly driven by non-resonant parts of the magnetic perturbations. This is valid in part since the resonant components of the perturbations applied by external coils are largely shielded by plasmas thus the non-resonant components penetrate deeply into plasmas [10]. However, the non-resonant components produce a small amount of NTV by themselves even though they can drive strong NTV by interacting with electric precession.

When we consider the actual variation in the field strength δB on a flux surface in the zero electric precession condition, NTV is dominated by its resonant component. We show the clear resonant nature of the NTV by directly applying each harmonics of the actual variation in the field strength to each flux surface. Here the magnetic perturbations $\delta B/B_0 = \delta_{mn}(\psi_n)\cos(m\theta - n\varphi)$ with $\delta_{mn}(\psi_n) = 0.02\psi_n^2$ are applied to a background plasma of $\nu_* \sim 1.0$ in Ref. [4]. Fixing the toroidal mode number as $n = 3$, the poloidal mode number is varied by $m = 6, 7, 8$ to change the resonant mode. The $\vec{E} \times \vec{B}$ rotation is set to be zero so that the toroidal rotation effects excluded in the following calculation.

As shown in Fig. 2(a), strong NTV peaks appear nearby the resonant flux surfaces at $q = 6/3, 7/3, 8/3$ corresponding to the applied poloidal mode number. The peak flux surface is shifted by the applied mode, and the NTV is dominated by the resonant perturbation. On the other hand, NTVs rapidly drop at the off-resonant flux surfaces, indicating a clear resonant nature of the magnetic braking driven by NTV. Note much stronger torques are found at the edge rather than the core in spite of off-resonances which is consistent with the theoretical prediction $\tau_\varphi \propto (\delta B)^2$. Fig. 2(b) shows the time evolutions of the peak NTV torques in Fig. 2(a). The calculated NTVs reach quasi-steady states in few collision times, which reveals a good convergence feature of POCA simulation. The NTV values obtained from the simulation are the long-time averages in the quasi-steady phase.

Overall trend of NTV profiles by POCA shows consistent agreements with the

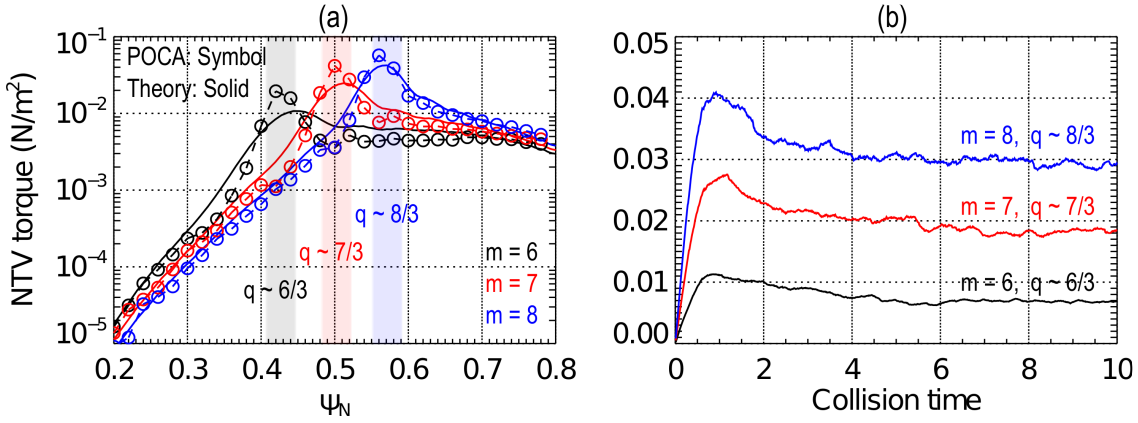

Figure 2. (a) NTV torque profiles by ($m = 6, 7, 8, n = 3$) modes. Strong NTV peaks appear at the resonant flux surfaces where $q = 6/3, 7/3, 8/3$ for each poloidal mode number. (b) Time evolutions of the peak NTV torques. The calculated torques approach quasi-steady states in few collision times.

combined theory in the high aspect-ratio and the low β plasmas as shown. The amplitudes also agree well within a factor of 2, confirming the validity of δf calculation using POCA.

3. Reconstruction of perturbed magnetic field δB for particle simulation

As previously described, an accurate calculation of the perturbed magnetic field δB is one of the essential requirements for the precise estimation of the non-ambipolar transport and the NTV torque. In a practical experiment, δB can be computed as multi-harmonic Fourier series, and is much more complicated than an analytic expression. The δB can largely differ from a vacuum perturbed field δB_v, which is generally computed by a vacuum field approximation, due to a plasma response. As a resolution, we use IPEC, a well-known ideal perturbed equilibrium code, capable of computing δB with an ideal plasma response. Technically, POCA has been developed to read axisymmetric equilibria from 20 different formats from experimental and analytic solution, and non-axisymmetric perturbation from IPEC.

IPEC computes the perturbed magnetic field spectrum and gives the spectrum as following form

$$\begin{aligned}\delta B_{mn}(\psi_n) = &\sum a_{mn}\cos(m\theta - n\varphi) \\ &+ b_{mn}\sin(m\theta - n\varphi),\end{aligned} \tag{5}$$

where a_{mn} and b_{mn} are the coefficients of Fourier harmonics for each mode. However, a direct application of Eq. 5 is not efficient in the particle simulation since the δB in Eq. 5 contains strong peaks at the rational flux surfaces, as shown in Fig. 3. The peaks are caused by the ideal plasma responses excluding islands, and can give nonphysical impacts on the drift motion of the particles crossing the rational surfaces. Thus, we develop a fitting technique using Chebyshev polynomials to smooth the peaks. The

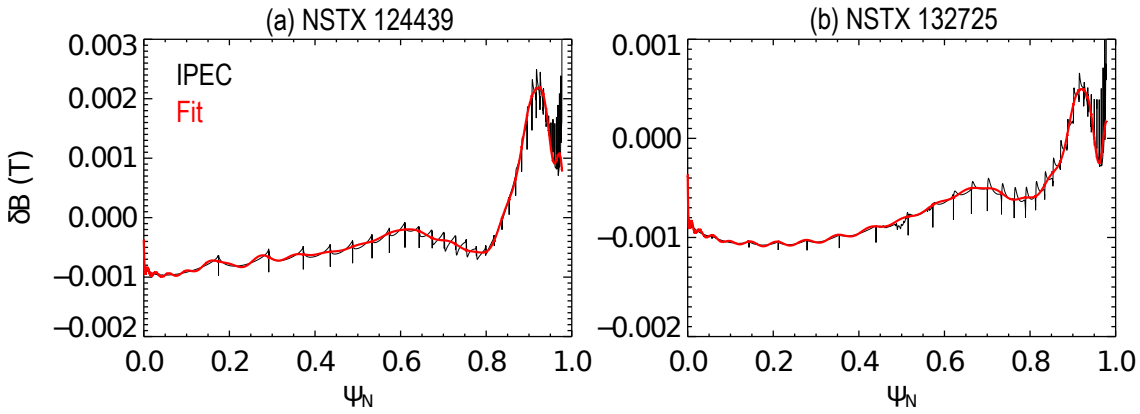

Figure 3. Comparison of non-axisymmetric magnetic field profiles between IPEC and fitting with Chebyshev polynomials for NSTX discharge (a) 124439 and (b) 132725. Profiles are taken at $(\theta, \varphi) = (0, 0)$ with $n_c = 20$. Fittings efficiently smooth the nonphysical peaks but reflect overall features of the original IPEC calculation well.

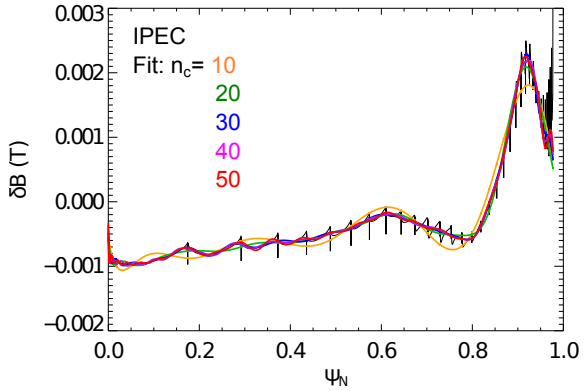

Figure 4. Sensitivity of Chebyshev fitting to the degree of polynomials. δB profiles for NSTX 124439 in Fig. 3(a) are taken.

fitting function of the δB is expressed as

$$\begin{aligned}\delta B_{mn}(\psi_n) = &\sum_m \sum_j^{n_c} a_j \cos[j \cos^{-1}(x)] \cos(m\theta - n\varphi) \\ &+ b_j \cos[j \cos^{-1}(x)] \sin(m\theta - n\varphi),\end{aligned} \tag{6}$$

where n_c is the degree of polynomials, a_j and b_j are the Chebyshev coefficients for each degree j, and $x = 2\psi_n - 1$.

Fig. 3 shows comparisons of the δB profiles between original IPEC result and fitting in the NSTX discharges, where the radial profiles are taken at $(\theta, \varphi) = (0, 0)$ with $n_c = 20$. One can notice that the fitted profiles reflect overall trend of complex field structure very well, even though the nonphysical peaks at the rational flux surfaces are effectively smoothed. The fitting function is sensitive to the degree of Chebyshev polynomials n_c as seen in Fig. 4, where each fitting curve is drawn for different n_c. A lower degree fitting roughly follows the original δB with wobbling, and shows a poor fitting quality at the edge with dense rational surfaces. On the other hand, high degree

gives a better fitting to the IPEC calculation, so that it follows very well the rapid δB changes at the rational surfaces and effectively smoothes the nonphysical peaks. The degree of polynomials of $n_c \geq 20$ is found to provide good resolutions for the examples, but this can depend on the discharge condition. Note higher degree usually guarantees an accurate fitting but requires longer simulation time. In the following experimental analyses, $n_c = 20$ is used to simultaneously satisfy the computational accuracy and efficiency.

4. NTV calculations in magnetic braking experiments

POCA applications are described in this section for magnetic braking experiments in DIII-D and NSTX. For the simulations, IPEC first computes the perturbed magnetic field δB with the ideal plasma response, and then POCA calculates the NTV using the δB from Eq. 6 with kinetic profile measurements for temperature, density and rotation. The electric potential profile in Eq. 3 is obtained from a radial force balance equation $\nabla p = eN(\vec{E}+\vec{u}\times\vec{B})$, which is given by measurements and not self-consistently calculated in the POCA simulation. It was from measured pressure and toroidal rotation, and neoclassical estimation of poloidal rotation in NSTX, while the poloidal rotation was also measured in DIII-D.

Note $\vec{E}\times\vec{B}$ precessions always exist in the practical plasmas and make the particle orbits much more complicated compared to the zero-$\vec{E}\times\vec{B}$ case. In particular, the bounce-harmonic resonance [21, 22], which is the resonance between the parallel bounce motions and the perpendicular $\vec{E}\times\vec{B}$ drift motion, is an important mechanism to drive NTV in the finite $\vec{E}\times\vec{B}$ as predicted in the theory [14]. This bounce-harmonic effect is automatically included in the POCA simulation by the guiding-center drift motions so that the orbit closing and evolution by $\vec{E}\times\vec{B}$ are realistically taken into account.

4.1. DIII-D discharge in the conventional aspect-ratio

A QH-mode discharge 145117 in DIII-D tokamak is selected to validate the NTV calculation using POCA. The QH-mode is believed to be accessible by strong rotational shears at the edge, and non-axisymmetric magnetic perturbations can be used to produce them [23]. For this discharge, non-resonant $n = 3$ non-axisymmetric magnetic perturbations were applied using I-coil and C-coil to the NBI-heated plasma ($I_P = 1.1$ MA, $B_T = 1.95$ T), so the net-NBI torque at the ITER-relevant level was achieved with the magnetic braking by the NTV torque [24].

Total NTV torque in the discharge was measured using an angular momentum balance equation and estimated at ~ 3 Nm, as described in Ref. [24]. There is no measurement for the NTV profile in this discharge, therefore the total NTV is used for a comparison with the simulation. Fig. 5 presents the calculation results of NTV torque profile by POCA and the combined NTV formula, and shows a good agreement in the profile and amplitude. The POCA calculation predicts stronger NTV at the

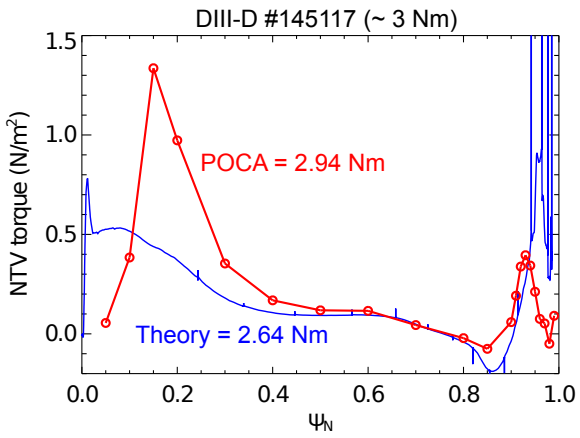

Figure 5. NTV calculation for DIII-D discharge 145117. POCA (red) and the combined theory (blue) agree well in the NTV profile. Both calculations provide a reasonable prediction in total NTV torque (2.94 Nm by POCA, 2.64 Nm by theory), which is estimated at ~ 3 Nm in the experiment.

core and weaker NTV at the edge than the theory, but the overall trend is consistent with each other. Both calculations agree well with the experimental estimation for the total NTV torque, i.e. 2.94 Nm by POCA and 2.64 Nm by theory, indicating the successful application of the developed particle simulation. Strong peaks in the theory calculation in Fig. 5 are due to the amplification of NTV at the rational surfaces by $\tau_\varphi \propto (\delta B)^2$ since the theory uses δB from IPEC. It is not clear why a NTV peak around $\psi_N = 0.2$ appears in the POCA simulation. A possible candidate for this peak is an effect by passing particles as reported in Ref. [25], since analytic calculation considers only trapped particles. Note that the combined NTV calculation is updated with the higher resolutions and thus improved integrations on both spatial and velocity space compared to Ref. [24].

The combined NTV theory can give a good qualitative guide, and even a good quantitative prediction for the NTV in the conventional aspect-ratio and slow/intermediate rotation frequencies ($\Omega_\phi \sim 10$ krad/s in this discharge). It should be noted that the combined theory calculation indicates $\ell = 0$ class particles are dominant for driving NTV in the analyzed discharge, where ℓ is the digit representing the bouncing class of particles. This means the bounce-harmonic resonance effect on the NTV is not strong. However, it has been found that POCA predicts stronger bounce-harmonic resonances and thereby stronger NTV than the theory in the fast rotating plasmas [26]. We expect that the analytic NTV theory becomes less precise in fast rotating plasmas due to strong distortions in particle orbits by fast precession. More analyses on the rotation effects needs to be performed in the DIII-D to check a validity of the theory in the conventional aspect-ratio.

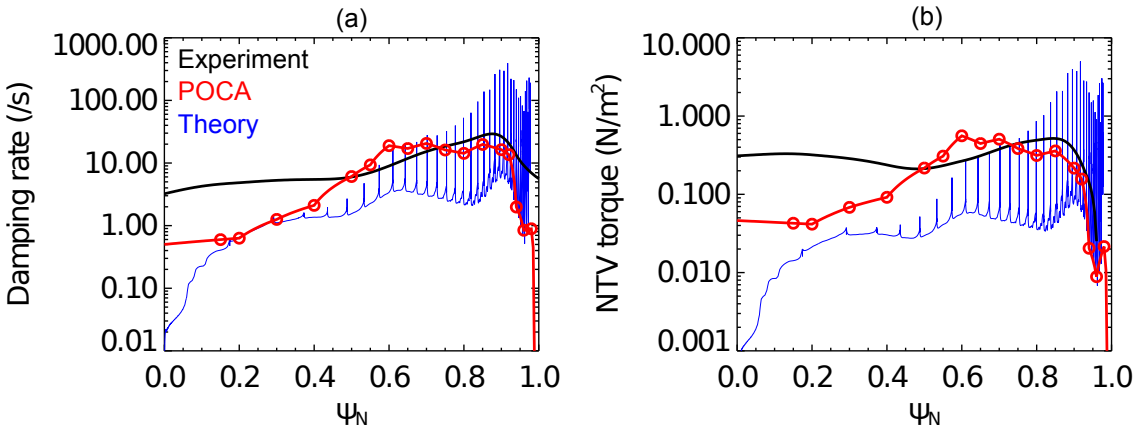

Figure 6. Comparison of (a) rotational damping rate and (b) NTV torque profile between measurement (black), POCA (red) and theory (blue) for NSTX discharge 124439. Total NTV torque is measured at 3.5 Nm, and agrees well with 2.7 Nm from POCA.

4.2. NSTX discharges in the low aspect-ratio

Two magnetic braking discharges 124439 and 132729 for NSTX were analyzed using POCA. Axisymmetric equilibriums are reconstructed using LRDFIT [27]. The toroidal rotation speed u_φ is measured by charge exchange recombination spectroscopy (CHERS) based on carbon impurities, assuming the CHERS represents the main ion rotation. The poloidal rotation is neglected in the simulations due to the fast toroidal rotation in the selected discharges.

For the NSTX discharges, NTV torque profiles were measured from toroidal rotation changes by the magnetic braking, as described in Ref [28]. In the discharge 124439, where $\kappa = 2.3$, $I_p = 0.8$ MA, and $B_T = 0.45$ T in the lower single null configuration, the toroidal rotation was observed to damp and relax to a different rotational equilibrium after $n = 3$ magnetic braking was fully applied by EF/RWM coils. Particle transport was not changed even though the non-axisymmetric fields produce a strong momentum transport, and it was clearly indicated that the damping is purely driven by the $n = 3$ magnetic braking [28].

A reference discharge, where the plasma is identical except the magnetic braking, is useful to estimate the toroidal rotational damping rate $\nu_{\rm damp}$. The rotational damping rate can be measured by calculating the rotation changes of the target discharge compared to the reference shot. A short time period after turning on EF/RWM coils is considered so that an exponential decay of the rotation can be linearized [28]. Then, the NTV is calculated from the damping rate using

$$\tau_\varphi \approx \nu_{\rm damp} u_N^\varphi RMN, \tag{7}$$

where M is the mass of a species, N is the density, R is the major radius, and u_N^φ is the neoclassical toroidal flow. The neoclassical toroidal flow is defined by

$$u_N^\varphi \equiv u_\varphi + C_N \left| \frac{1}{eZ} \frac{dT}{d\chi} \right|, \tag{8}$$

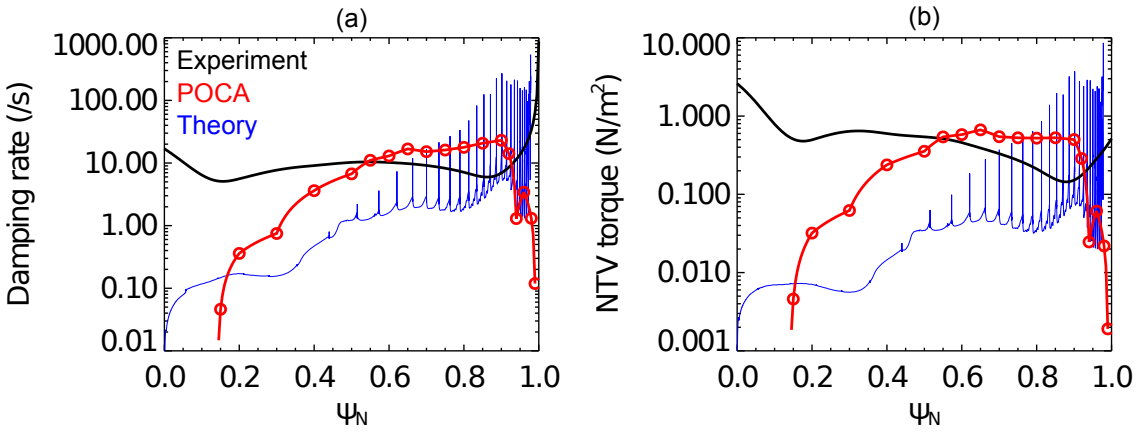

Figure 7. Comparison of (a) the rotational damping rate and (b) the NTV torque profile among measurement (black), POCA (red), and theory(blue) for NSTX discharge 132729.

where χ is the poloidal flux function. The second term of Eq. 8 represents a neoclassical offset flow with $C_N \approx 3.5$ for $1/\nu$ regime, $C_N \approx 0.92$ for $\nu_-\sqrt{\nu}$ regime, and $C_N \approx 2.0$ for combined regime [12, 14]. The offset flow has not been measured in NSTX, so it is analytically calculated using Eq. 8.

Fig. 6(a) shows a comparison of the rotational damping rate between the measurement and POCA, drawn together with a prediction by the combined theory. The POCA calculation shows reasonable agreement with the observed damping profile even though $\nu_{\rm damp}$ by POCA is weaker at $\psi_N < 0.4$ and stronger at the outer region at $0.4 < \psi_N < 0.9$. Theory prediction is only valid within an order of magnitude in the NSTX. Fig. 6(b) shows the NTV profiles by POCA and the measurement. Similarly, POCA indicates weaker NTV at inner region and stronger at outer region. POCA gives 2.7 Nm for the total NTV torque which is more consistent with the experimental value 3.5 Nm than the combined theory prediction of 0.55 Nm. Note that the combined NTV calculation here is updated with the higher resolutions and thus improved integrations on both spatial and velocity space, and also with the flow offset for the damping rate, compared to Ref. [28]. The conclusion in Ref. [28] was that the combined NTV based on Lagrangian δB in IPEC improved the consistency between theory and experiment within an order of magnitude but the accuracy is still not sufficient to predict the damping rates in details. In this work, POCA gives another significant improvement quantitatively, at least for the total NTV.

Another NSTX discharge 132729, where $I_p = 1.1$ MA and $B_T = 0.55$ T, was analyzed for the NTV in the same manner. For this discharge, 750 A of current was run in the NSTX to produce strong $n = 3$ magnetic braking, as described in Ref. [29]. Fig. 7 presents comparisons of the damping rate and NTV torque profiles for 132729. Discrepancies are found in both profiles, where POCA predicts weaker NTV at the inner and edge region and stronger NTV elsewhere. The discrepancies in the profiles are more significant at the core, which might be caused by experimental and

numerical uncertainties as will be discussed in the next section. However, one can still find a better quantitative agreement for the total NTV torque due to sub-dominant contribution of the core to the total torque; POCA gives 3.5 Nm and the experiment 5.1 Nm. Theory still largely underestimate the total torque at 0.44 Nm. One can notice that only measurement shows large NTV at the edge unlike theory and simulation in this discharge, while NTV drops at the edge are consistently found in Figs. 5 and 6. This could be due to relatively unstable toroidal rotation measurement in the discharge, which also might cause an abnormally large NTV at the core in Fig. 7.

It is notable that the NSTX experiment has many differences compared to the DIII-D configuration, which result in the large discrepancies between the theory and the simulation. Theoretical approximations such as the large aspect-ratio expansion and the zero-orbit-width assumption become crucial and invalid for NSTX due to the low aspect-ratio and weak magnetic field configurations. In addition, the bounce-harmonic resonance effects become stronger than theory prediction when the rotation is fast in NSTX since particle transport by bounce-harmonic resonances can be largely underestimated without finite-orbit-width [26]. Passing particle effects excluded in theory have also non-negligible contributions on stronger NTV predicted by POCA simulations even in the large aspect-ratio [25]. Thus, the combined analytic theory can be reliable only within an order of magnitude in quantity. However, the POCA simulation provides an improved prediction in NSTX by eliminating such approximations.

5. Issues for improving NTV prediction

There are still issues to further improve the predictability and the understanding of NTV, even though the particle simulations have showed improved predictions over analytic theory. There are uncertainties and room for improvement in measuring the NTV from the toroidal angular momentum balance and/or the toroidal rotation diagnostics. First, separate transport calculations such as TRANSP analysis in Ref. [24] are required in order to obtain the total NTV from the toroidal angular momentum equation, and they contain their own uncertainties. For instance, the intrinsic torque term in the equation can be a source of error, and the profile is difficult to measure. Second, the damping rate measured by carbon ion rotation using CHERS can be different from that of main ion due to a different responding time to the non-axisymmetric perturbations. Also, an intrinsic assumption $u_\varphi \approx u_{\mathrm{carbon}}$ needs to be verified. Third, neoclassical offset flow should be measured. When estimating NTV torque profile from the measured damping rate, theoretically calculated neoclassical offset flow was used due to the absence of measurements. Generally, the offset flow can be strong at the H-mode edge due to a steep temperature gradient, so it can greatly enhance the NTV value at the edge. If one ignores the offset flow in the neoclassical toroidal flow in Eq. 8, Eq. 7 gives reduced torques in the edge and smaller total values of 1.5 Nm for 124439 and 2.36 Nm for 132729. This implies the importance of offset rotation in the NTV

measurement. Thus, more robust diagnostics for the toroidal rotation and offset flow are necessary to eliminate such uncertainties.

For the simulation, it should be noted that the ideal perturbed equilibria can fail in the high β plasmas and strong NTV braking, as in the NSTX discharges. The validity of the ideal perturbed equilibria has been theoretically discussed using dimensionless parameters in Ref. [5]; $s \equiv -\delta W/\delta W_v$ and $\alpha \equiv -T_\varphi/2N\delta W_v$ with δW the total energy, δW_v the required energy to produce the same perturbation without plasma, and T_φ the total NTV torque. This theory indicates that the ideal perturbed equilibria can be valid when $|s| > |\alpha|$, corresponding to weak NTV. Otherwise, a shielding effect associated with the toroidal toque becomes crucial to prevent a penetration of the perturbed magnetic fields. In this sense, the δB from the ideal perturbed equilibria gives an inconsistent NTV by the ignorance of such shielding effects.

The studied NSTX discharges satisfy $|s| > |\alpha|$, indicating the presented NTV based on ideal δB is globally valid and explaining the quantitative agreements. However, the NTV effects on perturbed equilibria in fact can occur differently depending on locations. The strong NTV spikes around the rational surfaces can induce currents associated with NTV and can change the field penetration and consequently δB in the perturbed equilibrium. These local NTV effects should be considered particularly at the edge, which is generally dense with the rational surfaces as shown in Fig. 6 and 7. The self-consistent calculation of δB including the non-ideal plasma response will eventually be required to obtain self-consistent predictions of the perturbed equilibria and thereby the NTV transport. It can be achieved from a general perturbed equilibrium code solving 3D force balance with the perturbed anisotropic tensor pressure.

6. Conclusions

A Particle Orbit Code for Anisotropic pressures, POCA has been developed for the accurate calculation of δf by guiding-center drift given non-axisymmetric equilibria. NTV analysis has been carried out using analytic and practical non-axisymmetric magnetic field perturbations. Simulation with the analytic perturbation clearly indicates the strong resonant nature of NTV torque, consistently with the combined NTV theory. POCA applications to magnetic braking experiments in DIII-D and NSTX also show better quantitative predictions than analytic calculations, even though there remain discrepancies in the NTV profiles, especially for NSTX discharges as in Fig. 7. More robust estimation of NTV is necessary in the future, and it can be achieved by dedicated rotation measurement and integrated momentum transport analysis with reliable torque sources.

Theoretical and numerical uncertainties could be overcome through general perturbed equilibria. The calculation based on ideal perturbed equilibria breaks down in the high β plasmas and in strong magnetic braking cases. Penetration of the perturbed field into the plasma can be significantly changed by the non-ideal plasma response associated with the strong local NTV. Thus, the self-consistent δB by a general

perturbed equilibria is required to achieve more precise NTV prediction. The self-consistent NTV calculation can be accomplished throughout an integrated calculation of the transport and the General Perturbed Equilibrium Code (GPEC), which is actively under way.

Acknowledgments

This work was supported by DOE Contract No. DE-AC02-09CH11466 (PPPL) and No. DE-FC02-04ER54698 (GA).

[1] A. A. Galeev, R. Z. Sagdeev, H. P. Furth, and M. N. Rosenbluth. Plasma diffusion in a toroidal stellarator. *Phys. Rev. Lett.*, 22:511, 1969.

[2] R. J. Goldston, R. B. White, and A. H. Boozer. Confinement of high-energy trapped particles in tokamaks. *Phys. Rev. Lett.*, 47:647, 1981.

[3] A. H. Boozer. Enhanced transport in tokamaks due to toroidal ripple. *Phys. Fluids*, 23:2283, 1980.

[4] K. Kim, J.-K. Park, G. J. Kramer, and A. H. Boozer. δf monte carlo calculation of neoclassical transport in perturbed tokamaks. *Phys. Plasmas*, 19:082503, 2012.

[5] A. H. Boozer. Error field amplification and rotation damping in tokamak plasmas. *Phys. Rev. Lett.*, 86:5059, 2001.

[6] S. A. Sabbagh, A. C. Sontag, J. M. Bialek, D. A. Gates, A. H. Glasser, J. E. Menard, W. Zhu, M. G. Bell, R.E. Bell, A. Bondeson, C. E. Bush, J. D. Callen, M.S. Chu, C. C. Hegna, S. M. Kaye, L. L. Lao, B. P. LeBlanc, Y. Q. Liu, R. Maingi, D. Mueller, K. C. Shaing, D. Stutman, K. Tritz, and C. Zhang. Resistive wall stabilized operation in rotating high beta nstx plasmas. *Nucl. Fusion*, 46:635, 2006.

[7] A. M. Garofalo, K. H. Burrell, J. C. DeBoo, J. S. deGrassie, G. L. Jackson, M. Lanctot, H. Reimerdes, M. J. Schaffer, W. M. Solomon, and E. J. Strait. Observation of plasma rotation driven by static nonaxisymmetric magnetic fields in a tokamak. *Phys. Rev. Lett.*, 101:195005, 2008.

[8] T. E. Evans, R. A. Moyer, P. R. Thomas, J. G. Watkins, T. H. Osborne, J. A. Boedo, E. J. Doyle, M. E. Fenstermacher, K. H. Finken, R. J. Groebner, M. Groth, J. H. Harris, R. J. La Haye, C. J. Lasnier, S. Masuzaki, N. Ohyabu, D. G. Pretty, T. L. Rhodes, H. Reimerdes, D. L. Rudakov, M. J. Schaffer, G. Wang, and L. Zeng. Suppression of large edge-localized modes in high-confinement diii-d plasmas with a stochastic magnetic boundary. *Phys. Rev. Lett.*, 92:235003, 2004.

[9] S. A. Sabbagh, R. E. Bell, J. E. Menard, D. A. Gates, A. C. Sontag, J. M. Bialek, B. P. LeBlanc, F. M. Levinton, K. Tritz, and H. Yuh. Active stabilization of the resistive-wall mode in high-beta, low-rotation plasmas. *Phys. Rev. Lett.*, 97:045004, 2006.

[10] J. D. Callen. Effects of 3d magnetic perturbations on toroidal plasmas. *Nucl. Fusion*, 51:094026, 2011.

[11] K. C. Shaing and J. D. Callen. Neoclassical flows and transport in non-axisymmetric toroidal plasmas. *Phys. Fluids*, 26:3315, 1983.

[12] K. C. Shaing. Magnetohydrodynamic-activity-induced toroidal momentum dissipation in collisionless regimes in tokamaks. *Phys. Plasmas*, 10:1443, 2003.

[13] K. C. Shaing, P. Cahyna, M. Becoulet, J.-K. Park, S. A. Sabbagh, and M. S. Chu. Collisional boundary layer analysis for neoclassical toroidal plasma viscosity in tokamaks. *Phys. Plasmas*, 15:082506, 2008.

[14] J.-K. Park, A. H. Boozer, and J. E. Menard. Non-ambipolar transport by trapped particles in tokamaks. *Phys. Rev. Lett.*, 102:065002, 2009.

[15] A. J. Cole, J. D. Callen, W. M. Solomon, A. M. Garofalo, C. C. Hegna, M. J. Lanctot, H. Reimerdes, and the DIII-D Team. Peak neoclassical toroidal viscosity at low toroidal rotation in the diii-d tokamak. *Phys. Plasmas*, 18:055711, 2011.

[16] J.-K. Park, A. H. Boozer, and A. H. Glasser. Computation of three-dimensional tokamak and spherical torus equilibria. *Phys. Plasmas*, 14:052110, 2007.

[17] M. Sasinowski and A. H. Boozer. A δf monte carlo method to calculate plasma parameters. *Phys. Plasmas*, 4:3509, 1997.

[18] R. B. White. Canonical hamiltonian guiding center variables. *Phys. Fluids B*, 2:845, 1990.

[19] J. D. Williams and A. H. Boozer. δf method to calculate plasma transport and rotation damping. *Phys. Plasmas*, 10:103, 2003.

[20] S. Satake, J.-K. Park, H. Sugama, and R. Kanno. Neoclassical toroidal viscosity calculations in tokamaks using a δf monte carlo simulation and their verifications. *Phys. Rev. Lett.*, 107:055001,

2011.

[21] R. Linsker and A. H. Boozer. Banana drift transport in tokamaks with ripple. *Phys. Fluids*, 25:143, 1982.

[22] H. E. Mynick. Generalized banana-drift transport. *Nucl. Fusion*, 26:491, 1986.

[23] A. M. Garofalo, W. M. Solomon, J.-K. Park, K. H. Burrell, J. C. DeBoo, M. J. Lanctot, G. R. McKee, H. Reimerdes, L. Schmitz, M. J. Schaffer, and P. B. Snyder. Advances towards qh-mode viability for elm-stable operation in iter. *Nucl. Fusion*, 51:083018, 2011.

[24] K. H. Burrell, A. M Garofalo, W. M. Solomon, M. E. Fenstermacher, T. H. Osborne, J.-K. Park, M. J. Schaffer, , and P. B. Snyder. Reactor-relevant quiescent h-mode operation using torque from non-axisymmetric, non-resonant magnetic fields. *Phys. Plasmas*, 19:056117, 2012.

[25] S. Satake, J.-K park, H. Sugama, and R. Kanno. Drift-kinetic simulation studies on neoclassical toroidal viscosity in tokamaks with small magnetic perturbations. In *Proceedings of 24th IAEA Fusion Energy Conference*. IAEA, San Diego, 2012.

[26] K. Kim, J.-K. Park, and A. H. Boozer. Numerical verification of bounce harmonic resonances in neoclassical toroidal viscosity for tokamaks. 2012. Submitted.

[27] J. E. Menard, R. E. Bell, D. A. Gates, S. M. Kaye, B. P. LeBlanc, F. M. Levinton, S. S. Medley, S. A. Sabbagh, D. Stutman, K. Tritz, and H. Yuh. Observation of instability-induced current redistribution in a spherical-torus plasma. *Phys. Rev. Lett.*, 97:095002, 2006.

[28] J.-K. Park, A. H. Boozer, J. E. Menard, S. P. Gerhardt, and S. A. Sabbagh. Shielding of external magnetic perturbations by torque in rotating tokamak plasmas. *Phys. Plasmas*, 16:082512, 2009.

[29] S. P. Gerhardt, J. E. Menard, J.-K. Park, R. Bell, D. A. Gates, B. P. Le Blanc, S. A. Sabbagh, and H. Yuh. Observation and correction of non-resonant error fields in nstx. *Plasma Phys. Control. Fusion*, 52:104003, 2010.

The Princeton Plasma Physics Laboratory is operated
by Princeton University under contract
with the U.S. Department of Energy.

Information Services
Princeton Plasma Physics Laboratory
P.O. Box 451
Princeton, NJ 08543

Phone: 609-243-2245
Fax: 609-243-2751
e-mail: pppl_info@pppl.gov
Internet Address: http://www.pppl.gov